DOI: 10.1002/chem.200700355

A Phosphine-Mediated Through-Space Exchange Coupling Pathway for Unpaired Electrons in a Heterobimetallic Lanthanide–Transition Metal Complex

Ritu Raturi,[a] Julie Lefebvre,[b] Daniel B. Leznoff,[b] Bruce R. McGarvey,[a] and Samuel A. Johnson*[a]

Abstract: The reaction of $P(CH_2OH)_3$ with methyl anthranilate $NH_2C_6H_4$-2-CO_2Me produced the ligand precursor $P(CH_2NHC_6H_4$-2-$CO_2Me)_3$ (**1**). The reaction of **1** with $[Y\{N(SiMe_3)_2\}_3]$ produced hexadentate yttrium complex $[Y\{P(CH_2NC_6H_4$-2-$CO_2Me)_3\}]$ (**2**), in which the metal centre is coordinated by three amido donors and the three carbonyl oxygen atoms of the ester groups. The $^{31}P\{^1H\}$ NMR spectrum features $^1J_{Y,P} = 15$ Hz, and DFT calculations demonstrate that through-space interaction between the minor lobe of the phosphine lone pair and the yttrium centre allows a large Fermi contact contribution to this spin coupling constant. The EPR spectrum of the analogous paramagnetic Gd complex $[Gd\{P(CH_2NC_6H_4$-2-$CO_2Me)_3\}]$ (**3**) can be modelled by using a B_{20} crystal field parameter of $\pm 0.19\ cm^{-1}$. Heterodinuclear complexes were prepared by the reactions of **1** and **3** with [5,10,15,20-tetrakis(4-methoxyphenyl)porphinato]-cobalt(II), by binding of the phosphine lone pair to the d^7 cobalt centre. The solid-state EPR spectrum of the heterodinuclear yttrium complex **4** exhibits large superhyperfine coupling to the phosphorus nucleus, indicative of an $S = 1/2$ complex in which the unpaired electron resides in the cobalt d_{z^2} orbital directed at the phosphine donor. The magnetic susceptibility of the heterodinuclear Gd–Co complex **5** demonstrates that through-space antiferromagnetic coupling occurs between unpaired electrons on the gadolinium and cobalt centres.

Keywords: heterometallic compounds · lanthanides · magnetic properties · N,O ligands · through-space interactions

Introduction

Essential to the design of molecule-based magnets,[1,2] including single-molecule magnets, is the ordering of spins via exchange coupling.[3] Progress in this area demands synthetic approaches to the design of intricate architectures, which can include macromolecular polynuclear complexes, 1D wires and 2D or 3D networks.[2,4] Typically, the same bonding interactions that assemble these complexes and networks are also responsible for transmission of exchange coupling, frequently by a superexchange pathway. Single atoms bridging metal centres often perform this role, but larger π-conjugated bridging ligands are also capable of propagating exchange coupling, and the cyano donor in particular has recently revolutionised the design of magnetic network structures[5] and single-molecule magnets.[6] An increase in the variety of ligands that could facilitate a building-block approach[7] to magnetic materials would be a boon to this field, and in particular building blocks with at least axial symmetry would aid in the modelling of magnetically anisotropic systems.

We have shown how formally trianionic tripodal triamidophosphine ligands such as $P(CH_2NPh)_3$ can be used to generate both polynuclear[8] and heterobimetallic complexes,[9] as depicted in Figure 1. If exchange coupling occurs between the metal centres labelled M and M′ in paramagnetic heterobimetallic analogues, these $P(CH_2NPh)_3M$ moieties could act as valuable building blocks. Due to the ubiquity of phosphine donors in coordination chemistry, it should prove

[a] R. Raturi, Prof. B. R. McGarvey, Prof. S. A. Johnson
Department of Chemistry & Biochemistry
University of Windsor
401 Sunset Ave, Windsor ON, N9B 3P4 (Canada)
Fax: (+1) 519-973-7098
E-mail: sjohnson@uwindsor.ca

[b] J. Lefebvre, Prof. D. B. Leznoff
Department of Chemistry, Simon Fraser University
8888 University Drive, Burnaby BC, V5A 1S6 (Canada)

Supporting information for this article is available on the WWW under http://www.chemeurj.org/ or from the author.

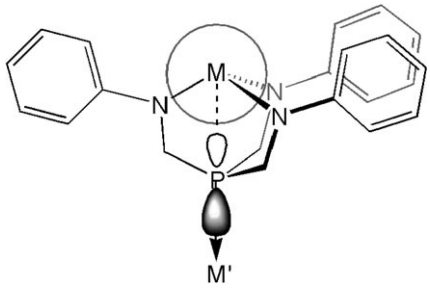

Figure 1. Through-space and through-bond interactions in tripodal complexes of $P(CH_2NPh)_3$ with metal centres M and M′ via the minor and major lobes, respectively, of the lone-pair orbital on phosphorus.

facile to utilize these complexes in the assembly of magnetic polynuclear complexes and modify them to generate extended networks. The four σ bonds separating M and M′ would seem to preclude any significant exchange coupling via this pathway, but the minor lobe of the phosphine lone pair extends towards metal centre M, which in theory could provide a unique combination of through-bond and through-space pathways for exchange coupling. The study of d–f heterodinuclear complexes of lanthanides and transition metals[10–13] is of current interest due to reports that the large magnetic anisotropies of the heavier lanthanides[14] can be utilised in the design of single-molecule magnets.[12,15] Herein we show how this through-space interaction can be utilised with paramagnetic metal centres to facilitate exchange coupling between M and M′, even in the difficult case where M is a lanthanide bearing core-like f electrons.

Results and Discussion

Synthesis of the ligand precursor: To achieve the goal of stable well-defined lanthanide building blocks, we sought to modify the tripodal triamido donors we had previously utilised to incorporate additional donors, due to the propensity of the trivalent lanthanides to assume high coordination numbers. The target ligand precursor $P(CH_2NHC_6H_4\text{-}2\text{-}CO_2Me)_3$ (**1**) was synthesised by reaction of $P(CH_2OH)_3$ with methyl anthranilate $H_2NC_6H_4\text{-}2\text{-}CO_2Me$ in toluene [Eq. (1)]. The water produced in this reaction was removed by azeotropic distillation with a Dean–Stark apparatus.[16] Solutions of **1** oxidize rapidly in air, and thus the solid product was stored in an inert-atmosphere glove box.

X-ray quality crystals of **1** were obtained by slow evaporation of a benzene/hexamethyldisiloxane solution. An ORTEP depiction of the solid-state molecular structure is shown in Figure 2. The structure features intramolecular hydrogen bonding between the carbonyl and amino groups. The positions of the three amino hydrogen atoms were refined by using isotropic thermal parameters. The sum of C-P-C angles is 298.31(2)°, which is typical for phosphine donors.

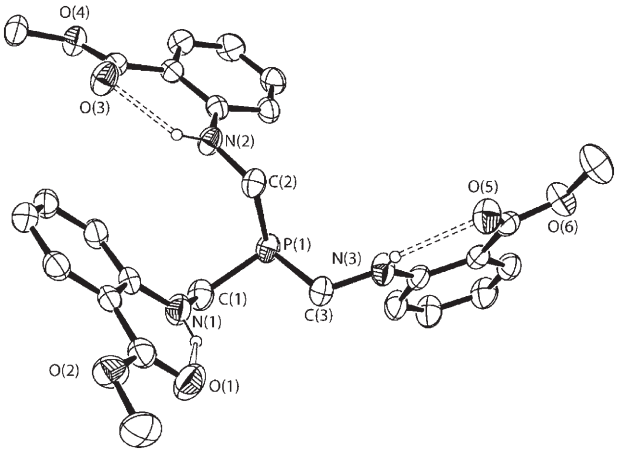

Figure 2. Solid-state structure of **1** as determined by X-ray crystallography. Hydrogen atoms are omitted for clarity, except those associated with N1, N2 and N3. Hydrogen-bonding interactions are shown as dashed lines. Selected bond angles [°]: C(1)-P(1)-C(2) 102.6213, C(1)-P(1)-C(3) 98.4414, C(1)-P(1)-C(3) 97.25(13).

Synthesis of a mononuclear yttrium complex: The similar ionic radius of Y^{III} to those of heavier lanthanides such as Gd^{III} prompted us to start our studies by preparing an yttrium complex of **1** as a diamagnetic model complex. Reaction of **1** with $[Y\{N(SiMe_3)_2\}_3]$ in toluene at room temperature [Eq. (2)] resulted in precipitation of rhombohedron-shaped yellow crystals of $[Y\{P(CH_2NC_6H_4\text{-}2\text{-}CO_2Me)_3\}]$ (**2**). The aromatic region of the ^1H NMR spectrum of **2** features four multiplets, which were assigned by a combination of 2D COSY and 2D NOESY spectroscopy. Analysis of the reaction mixture by ^1H and $^{31}P\{^1H\}$ NMR spectroscopy revealed that no side products were formed, other than the by-product $HN(SiMe_3)_2$.

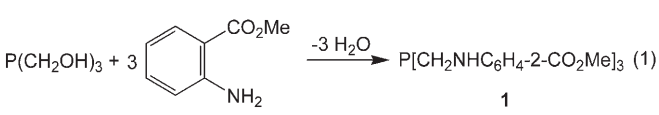

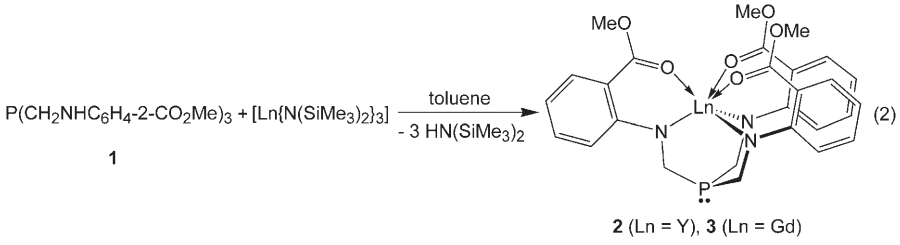

The solid-state molecular structure of **2** was determined by X-ray crystallography, and an ORTEP depiction is shown in Figure 3. Despite the collection of X-ray diffraction data on several crystals of **2** that appeared suitable for solid-state

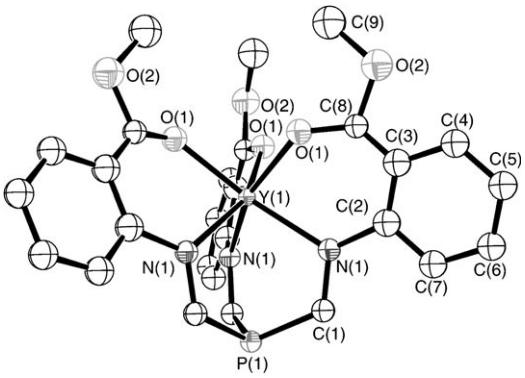

Figure 3. Solid-state molecular structure of **2** as determined by X-ray crystallography. Hydrogen atoms are omitted for clarity.

structure determination, twinning complicated solution of the structure. All atoms in the model structure were treated isotropically, and some restraints had to be used, which limited the accuracy of bond lengths and angles. Complex **2** has crystallographic C_3 symmetry, and features a six-coordinate Y centre chelated by the ligand amido donors and the carbonyl oxygen atoms of the ester groups. The phosphine lone pair is directed away from the metal centre and thus is available for donation to a second metal.

Through-space ^{31}P–^{89}Y coupling: The ^{31}P{^{1}H} chemical shift of **1** is $\delta = -33.6$ ppm, whereas for **2** the ^{31}P signal is observed at $\delta = -57.0$ ppm. This shift to higher field is unusual, because the increase in C-P-C angles upon coordination of a large metal centre such as Y should cause the opposite effect;[17] we have previously ascribed this unusual shift in related complexes to interactions of the minor lobe of the lone pair with the adjacent metal centre.[9]

Also notable in the ^{31}P{^{1}H} NMR of complex **2** is the observation of a 15 Hz coupling between yttrium (^{89}Y, $I = {}^{1}/_{2}$) and phosphorus. This $^{3}J_{P,Y}$ value is large considering that $^{1}J_{P,Y}$ values are typically in the range of 50–80 Hz,[18] and $^{2}J_{P,Y}$ values are typically 4–6 Hz, though values as large as 11 Hz have been reported in conjugated systems.[19] The largely ionic nature of bonding to Y suggests that $^{3}J_{P,Y}$ coupling constants should be smaller, due to smaller Fermi contact terms, but we could find no $^{3}J_{P,Y}$ values in the literature for comparison. This suggests that coupling between Y and P could be mediated by a through-space interaction. The X-ray data suggest an approximate Y···P distance of 3.36 Å, and the proximity of the P and Y atoms could allow a formally bonding interaction to occur between the minor lobe of the phosphorus lone pair and the metal centre.

Ab initio calculation with the DFT B3YLP method and DGDZVP basis sets was used to test this theory. This calculation predicts a $J_{P,Y}$ value of −11.2 Hz whose absolute value is close to the 15 Hz observed experimentally, and the Fermi contact term of −10.2 Hz predominates. The sign of this value is consistent with direct interaction between nuclei mediated by a pair of electrons and the opposite signs of the magnetogyric ratios for ^{31}P and ^{89}Y. The paramagnetic spin–orbit, dipolar and diamagnetic spin–orbit contributions to the coupling constant are all calculated to be much smaller than the Fermi contact term, with values of −0.8, −0.14 and −0.026 Hz, respectively. An analysis of the molecular orbitals predicted[20] from this calculation determined that only HOMO−3 has any significant overlap of density between P and Y, as required for a Fermi contact term. This orbital, which is primarily associated with the lone pair on phosphorus, is depicted in Figure 4. The minor lobe of the lone pair

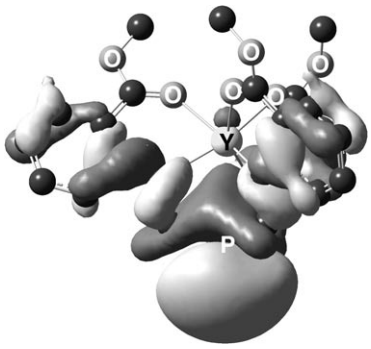

Figure 4. Depiction of the HOMO−3 orbital associated with the phosphorus lone pair, obtained from a DFT calculation, shown as the 0.01 e Å^{3} isosurface.

orbital clearly extends back towards the Y centre, and this allows for a through-space interaction.

Synthesis of a mononuclear gadolinium complex: The reaction of ligand precursor **1** with Gd[N(SiMe$_3$)$_2$]$_3$ produced the paramagnetic complex [Gd{P(CH$_2$NC$_6$H$_4$-2-CO$_2$Me)$_3$}] (**3**), as shown in Equation (2). Similar to the synthesis of **2**, yellow rhombohedron-shaped crystals precipitated from toluene. The crystal structures of **2** and **3** are isomorphous, and only small metric differences in the unit-cell parameters, due to the slightly larger size of Gd^{III}, were observed for this complex. As with complex **2**, this C_3-symmetric complex crystallised in a trigonal space group, difficulties associated with twinning complicated solution of this structure and connectivity could not be accurately determined.

The X-band EPR spectrum of a powdered sample of complex **3** was obtained at 77 K (Figure 5). The spectrum displays resonances from nearly zero field to 12500 G. The spectrum can be adequately modelled by using only a B_{20} value of ± 0.194 cm^{-1} (2080 G) and a g value of 1.994.[21] As would be expected for Gd^{III}, the B_{40} B_{43}, B_{60}, B_{63} and B_{66} crystal-field parameters were found to be much smaller than the B_{20} term, and attempts to fit these parameters did not produce a significantly better model of the experimental data; in fact more significant improvements in fit were obtained by modelling the line widths anisotropically. The zero-field splitting in **3** is almost an order of magnitude larger than has been reported for a related anionic bisphthalocyaninato gadolinium complex,[22] whose Dy, Tb[23] and Ho[24] analogues have been shown to behave as mono-

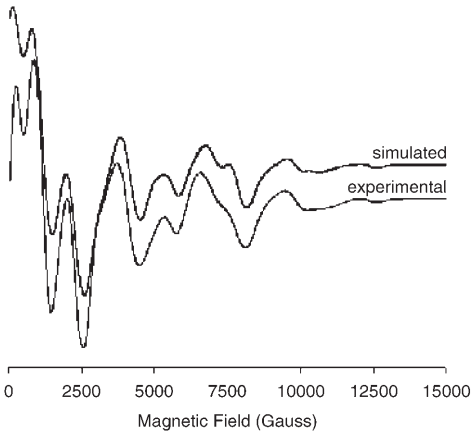

Figure 5. X-band EPR spectrum of a powdered sample of **3** at 77 K (lower trace) and a simulated spectrum (upper trace) with S = 7/2, $B_{20} = \pm 0.194\ cm^{-1}$ (± 2080 G), $g = 1.994$ and anisotropic line widths ($\| = 240$, $\perp = 360$ G).

nuclear single-molecule magnets due to the large ligand-induced zero-field splittings of their ground states. The approximate energy difference between the lowest and highest sublevels at zero field for complex **3** is $2.328\ cm^{-1}$; however, the relative sign of B_{20} cannot be determined from these EPR data, and thus it is not clear whether the $S = \pm 1/2$ or $S = \pm 7/2$ substates are lowest in energy.

Magnetic susceptibility of 3: The molar magnetic susceptibility χ_m of a powdered sample of complex **3** immobilised in eicosane was studied over the temperature range of 300.0–2.0 K. A plot of $\chi_m T$ versus T for **3** is provided in the Supporting Information. The $\chi_m T$ value of **3** at room temperature of $7.82\ cm^3 K mol^{-1}$ corresponds to the expected value for a Gd^{3+} ion at room temperature ($7.88\ cm^3 K mol^{-1}$), and is also in agreement with the value of $7.8\ cm^3 K mol^{-1}$ in toluene solution at room temperature determined by Evans's method. The magnitude of $\chi_m T$ for the powdered sample of **3** decreases slightly below 15 K, and reaches a value of $7.43\ cm^3 K mol^{-1}$ at 2 K. The modelled temperature dependence of $\chi_m T$ obtained using the negative value of the B_{20} crystal field value (i.e., $-0.194\ cm^{-1}$) obtained from the simulation of the EPR data is also provided in the Supporting Information. This model predicts a slight drop in $\chi_m T$ at low temperatures, as is observed, but the fit is not sufficient to determine the sign of B_{20}, because a similar decrease in $\chi_m T$ is predicted when a positive B_{20} value is used.

The calculated magnetic anisotropy at low temperatures for this magnitude of B_{20} is significant at temperatures below 20 K. At 1 K $\chi_{\| m} T$ and $\chi_{\perp m} T$ are predicted to be 15.74 and $3.31\ cm^3 K mol^{-1}$, respectively, when B_{20} is $-0.194\ cm^{-1}$. For the corresponding positive value of B_{20}, the $\chi_{\| m} T$ and $\chi_{\perp m} T$ values at 1 K are 2.60 and $10.07\ cm^3 K mol^{-1}$, respectively. The common assumption that Gd^{3+} in a crystal field can be treated as magnetically isotropic is clearly not valid in this system. Unfortunately, this complicates the modelling of this building block in heterobimetallic complexes, and the importance of this anisotropy in any observed exchange coupling is not readily ascertained. Regardless, the nearly temperature independent value of $\chi_m T$ in complex **3** facilitates the observation of spin–spin exchange coupling in heterobimetallic complexes prepared using this precursor.

DFT-calculated spin density: A DFT geometry optimization was performed on **3**, and the resultant calculated spin density is shown in Figure 6. The unpaired spins are primarily located on the Gd^{III} centre, which is expected due to the contracted nature of the f orbitals; however, some spin density of the opposite sign is found on the amido and carbonyl donor atoms. Only a very small contribution from unpaired spin density is found on the phosphorus atom or the carbon atoms. To use complex **3** as a magnetic building block, it is necessary to observe exchange coupling between the gadolinium centre and a transition metal bound to the available phosphine donor. The localised nature of the unpaired electrons on gadolinium necessitates a careful choice of transition metal to attach to the phosphine; it must be capable of delocalizing its unpaired electron density towards the gadolinium centre.

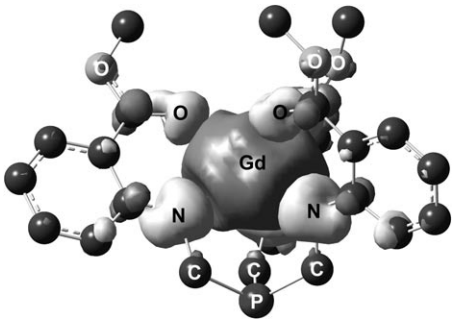

Figure 6. The 0.0001 e Å^3 isosurface of the calculated spin density for **3**.

Synthesis of heterobimetallic complexes: To demonstrate that through-space exchange coupling is viable in heterobimetallic complexes of these tripodal amidophosphine ligands, a transition metal complex must be attached to the phosphine donor that satisfies two requirements: Firstly, it must direct unpaired electron density towards the complexed gadolinium centre; secondly, it must have magnetic properties that are easy to model. We chose [Co(TPP)] (TPP = 5,10,15,20-tetrakis(4-methoxyphenyl)porphine) as the transition metal moiety, because it has a single unpaired electron in a nondegenerate orbital and thus should exhibit straightforward magnetism. Additionally, the SOMO in adducts of [Co(TPP)] is primarily the d_{z^2} orbital directed perpendicular to the plane of the [Co(TPP)] moiety, and thus should directly overlap with the phosphine donor orbital. Related five-coordinate phosphine adducts of Co^{II} porphyrins with diamagnetic phosphine donors are known.[25]

Complexes **2** and **3** react with [Co(TPP)] in toluene to provide brownish-purple crystalline solids which were iden-

tified as the heterobimetallic complexes [(TPP)Co{P($CH_2NC_6H_4$-2-$CO_2Me)_3$}Ln] [Ln = Y (**4**) or Gd (**5**); Eq. (3)].

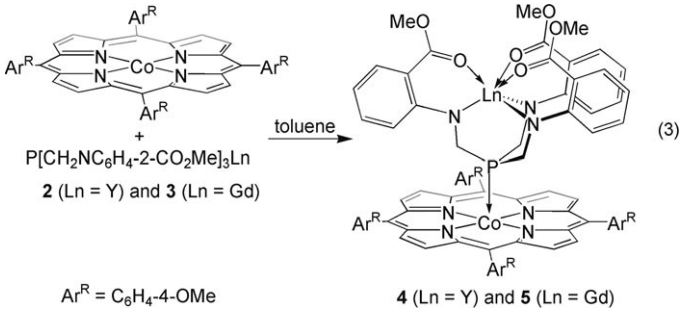

(3)

Single crystals of **4** and **5** were obtained by slow evaporation of saturated toluene solutions. The initial solubility of these complexes in toluene appears kinetic, as the resultant product has only modest solubility. The solid-state structures of **4** and **5** were determined by X-ray crystallography, and an ORTEP depiction of the solid-state molecular structure of **5** is shown in Figure 7. As anticipated, the triamido

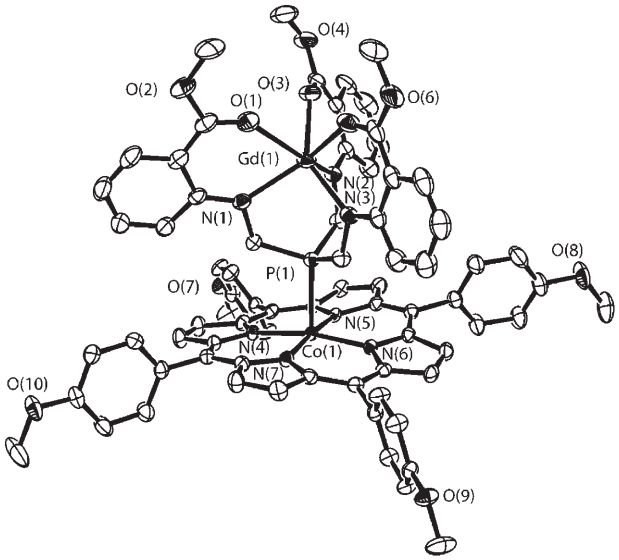

Figure 7. Solid-state molecular structure of **5** as determined by X-ray crystallography. Hydrogen atoms are omitted for clarity. Selected distances [Å]: P(1)–Co(1) 2.4128(9), Gd(1)–N(1) 2.325(3), Gd(1)–N(2) 2.332(3), Gd(1)–N(3) 2.336(3), Gd(1)···P(1) 3.2440(9).

donors chelate the lanthanide centre, and the phosphine lone pair is bound to the Co(TPP) moiety. Although **4** and **5** display slightly different metrical parameters, they are isostructural. These structures confirm the connectivity determined for the mononuclear complexes **2** and **3**; the tripodal ligand chelates via the amido donors and the carbonyl oxygen atoms. The Co–P bond length in complex **5** is 2.4128(9) Å. Reported Co^{II}–phosphine distances cover a large range, from as short as 2.2127(8) Å[26] to as long as 2.479(5) Å.[27] The relatively elongated Co–P bond length in **5** can be rationalised from a crystal-field theory argument that the lone unpaired electron in this d^7 species occupies the d_{z^2} orbital, which is directed towards the phosphine donor. The ionic radius of Gd^{III} is approximately 0.04 Å larger than that of Y^{III},[28] and this results in slightly different bond lengths between **4** and **5**. In **5**, the average Gd–N and Gd–O distances are 2.330(2) and 2.315(2) Å, respectively, whereas in **4** the average Y–N and Y–O bond lengths are 2.299(1) and 2.2771(9) Å, respectively. The P(1)···Y(1) distance of 3.2575(6) Å in **4** is less than 7% longer than the longest reported Y–P bond length of 3.045(2) Å,[29] although shorter Y–P bond lengths are more typical.[18,30] In comparison, the P(1)···Gd(1) distance of 3.2440(9) Å in **5** is actually shorter than the P(1)···Y(1) distance in **4**, which can be rationalised by the slightly larger size of the Gd^{III} ion requiring a greater strain in the ancillary ligand fro its accommodation. This assertion is confirmed by the slightly larger sum of C-P-C angles in **5** than in **4**, which are 326.70(26) and 324.69(17)°, respectively. These values are approximately 28° larger than the sum of C-P-C angles for ligand precursor **1**, which can be attributed primarily to the coordination of the large lanthanide ions.[9]

EPR spectra of 4 and 5: The X-band EPR spectrum of a frozen toluene solution of **4** was obtained at 77 K (Figure 8). It confirms that the complex remains a 1:1 adduct of **2** and

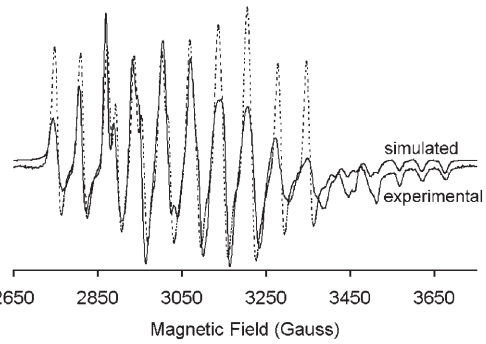

Figure 8. X-band EPR spectrum of a powdered sample of **4** at 77 K (solid line) and a simulated spectrum (dotted line, offset above) obtained by using $g_{\|} = 1.98$, $g_{\perp} = 2.21$, $A_{P\|} = 176$ G, $A_{P\perp} = 144$ G, $A_{Co\|} = 50$ G, $A_{Co\perp} = 63$ G.

[Co(TPP)] in solution, as well as the low spin $S = {}^1/_2$ nature of the complex. A simulated spectrum was obtained by considering the cobalt centre in **4** to have approximate axial symmetry and was fitted by using anisotropic $g_{\|}$ and $g_{\perp}$ values of 1.98 and 2.21, respectively. The simulation revealed that the phosphorus superhyperfine coupling constants $A_{P\|}$ and $A_{P\perp}$ of 176 and 144 G, respectively, are larger than the cobalt (^{59}Co, $I = 7/2$) hyperfine coupling constants $A_{Co\|}$ and $A_{Co\perp}$ of 50 and 63 G, respectively. The simulated spectrum is also shown in Figure 8. The EPR signal in solution at room temperature is a doublet due to superhy-

perfine coupling to ^{31}P, and A_{Co} cannot be resolved, which further confirms that in these adducts considerable unpaired electron density resides on the phosphine donor.

It has previously been shown[31] in related complexes that, by using third-order perturbation theory, the g values can be used to determine the energy separation of the $^2A_1$ ground state and the ^2E, $^4A_2$, and ^4E excited states in phosphine adducts of cobalt porphyrins. In this complex the lowest energy d orbitals should be the degenerate d_{xz} and d_{yz} orbitals, followed by the d_{xy} orbital and the singly occupied d_{z^2} orbital. The $d_{x^2-y^2}$ orbital is highest in energy and is unoccupied in the ground state. The c_1, c_3 and c_5 parameters are related to the $g_\parallel$ and $g_\perp$ values as shown in Equations (4) and (5). Here $c_1=\xi/(E[2E]-E[2A^1])$, where E[state] represents the energy of a given state and ξ is the one-electron spin–orbit coupling constant. The ^2E excited configuration results from promotion of an electron from doubly degenerate d_{xy} and d_{yz} to the d_{z^2} orbital. Similarly, parameters $c_3=\xi/(E[4E]-E[2A^1])$ and $c_5=\xi/(E[4A^2]-E[2A^1])$ correspond to the $^4A_2$ and ^4E configurations. With strong-field donors such as phosphines, the $^4A_2$ configuration, which results from promotion of an electron from the d_{xy} orbital to the $d_{x^2-y^2}$ orbital, is similar in energy to the ^4E state, which results from promotion of an electron from the doubly degenerate d_{xy} and d_{yz} orbitals to the $d_{x^2-y^2}$ orbital. This is because the d_{xz} and d_{yz} orbitals are relatively close in energy to the d_{xy} orbital, whereas the $d_{x^2-y^2}$ orbital is significantly higher in energy. The approximation that $c_3\approx c_5$ is therefore reasonable,[32,33] and a simplified expression for $g_\perp$ is obtained [Eq. (6)]. For complex **4** this analysis results in the values $c_1=0.039$ MHz and $c_3=0.11$ MHz, which is consistent with previously reported data for related complexes.[33]

$$g_\parallel = 2.0023 + 2\,c_3^2 - 3\,c_1^2 \tag{4}$$

$$g_\perp = 2.0023 + 6\,c_1 - 6c_1^2 + (2/3)\,c_3^2 + (8/3)\,c_5^2 - (4/3)\,c_3c_5 \tag{5}$$

$$g_\perp \approx 2.0023 + 6\,c_1 - 6\,c_1^2 + 2\,c_3^2 \quad (c_3 \approx c_5) \tag{6}$$

This analysis can be extended to the evaluation of the hyperfine and superhyperfine coupling constants.[31] The expressions for the hyperfine coupling constants $A_{Co\parallel}$ and $A_{Co\perp}$ are given in Equations (7) and (8) and can be used to estimate values of P, the dipolar term for the hyperfine coupling constant and K, the Fermi contact term. An expression for P under the assumption $c_3\approx c_5$ is shown in Equation (9). The P value for complex **4** was determined to be 683 MHz, which is very close to the value of 689 MHz for the free ion[34] and is indicative of primarily d_{z^2} spin density on the Co^{II} centre, as was anticipated. The value of K is −187 MHz. This analysis predicts that the sign of $A_{Co\perp}$ is negative.[31] Analysis of the superhyperfine coupling constants to ^{31}P allows evaluation of the contribution of the phosphorus 3s and 3p orbitals to the unpaired spin density on the phosphine donor.[33] This breakdown estimates that 12% of the unpaired spin density resides on the phosphine donor, with 4.5% associated with the phosphorus 3s orbital and 4.9% residing in the phosphorus 3p orbital.

$$A_{Co\parallel} = K + P[4/7 - (4/7)c_3 - (6/7)c_1 + (2/63)\,c_3^2 - (64/63)\,c_5^2 + (30/14)\,c_1^2 + (8/21)\,c_5c_3] \tag{7}$$

$$A_{Co\perp} = K + P[-2/7 + (2/7)\,c_3 + (45/7)\,c_1 + (12/63)\,c_3^2 + (40/63)\,c_5^2 - (57/14)\,c_1^2 - (34/21)\,c_5c_3] \tag{8}$$

$$P \approx (A_{Co\parallel} - A_{Co\perp})/[6/7 - (6/7)\,c_3 - (51/7)\,c_1 + (12/63)\,c_3^2 + (87/14)\,c_1^2] \tag{9}$$

A DFT calculation was performed on **4** using the solid-state structural data obtained by X-ray crystallography. The spin density predicted from this calculation is shown in Figure 9. Consistent with the EPR spectrum of **4**, this analysis reveals that considerable unpaired electron density resides on the phosphorus atom. Notably, this unpaired electron density extends back towards the Y centre, which should allow for through-space exchange coupling in complexes where Y is replaced by a paramagnetic lanthanide. The extensive delocalisation of the unpaired electron density onto the phosphorus atom and towards the yttrium centre can be rationalised by considering the nature of the SOMO, which can be approximated as an antibonding interaction between the phosphine lone pair, which has contributions from both the 3s and 3p orbitals of the phosphorus atom, and the d_{z^2} orbital of the cobalt centre. A simplified depiction of this interaction is also shown in Figure 9.

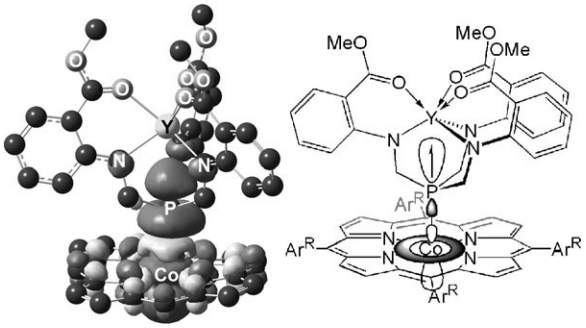

Figure 9. A depiction of the 0.0004 e Å^3 isosurface of the calculated spin density for heterodinuclear yttrium cobalt complex **4** (left) and a simplification of the antibonding interaction associated with the SOMO (right).

The X-band EPR spectrum of a powdered sample of **5** at 77 K is provided in the Supporting Information. The spectrum cannot be modelled to a reasonable fit by assuming no interaction between the Co^{II} and Gd^{III} centres for any combination of the B_{20} and B_{22} crystal-field parameters. The complete spin Hamiltonian for **5** would have to take into account the crystal-field splitting of the Stark substates and exchange coupling between the two metal centres. This is complicated by the presence of only pseudo-axial symmetry in **5**, as well as the significant exchange coupling interaction between the unpaired electrons associated with Co^{II} and Gd^{III}.

The exchange interaction is more easily estimated from the magnetic susceptibility data.

Magnetic properties of 4 and 5: The value of $\chi_m T$ for a toluene solution of complex **4** at 298 K was difficult to measure by Evans's method, due to the low solubility of **4** and the significant diamagnetic contribution cancelling the majority of the paramagnetic contribution to the susceptibility. The uncorrected value was determined to be 0.36 $cm^3 K mol^{-1}$, which is close to the value of 0.375 $cm^3 K mol^{-1}$ expected for a species bearing a single unpaired electron in a nondegenerate orbital, but after subtraction of the diamagnetic contribution a corrected value of $\chi_m T$ of 0.59 $cm^3 K mol^{-1}$ was obtained. The molar magnetic susceptibility of **4** was measured over the temperature range of 1.8–300 K in an applied magnetic field of 1 T, and $\chi_m T$ (corrected for a slight temperature-independent paramagnetism of 1.38×10^{-3} $cm^3 mol^{-1}$) was found to be independent of temperature, with a value of 0.39 $cm^3 K mol^{-1}$ at 1.8 K. The simplicity of the magnetism of this species renders the observation of exchange coupling in **5** facile, because in the absence of coupling negligible dependence of $\chi_m T$ on temperature is predicted.

At room temperature, the anticipated value of $\chi_m T$ for complex **5** is 8.26 $cm^3 K mol^{-1}$. This corresponds to the value for two uncoupled isolated ions Gd^{III} ($S=7/2$, $\chi_m T=$ 7.88 $cm^3 K mol^{-1}$) and Co^{II} ($S=1/2$, $\chi_m T=0.375$ $cm^3 K mol^{-1}$). The value of $\chi_m T$ for a solution of **5** in toluene at 298 K determined by Evans's method was 8.40 $cm^3 K mol^{-1}$, which is approximately that anticipated in the absence of coupling. The molar magnetic susceptibility of a powdered sample of complex **5** was measured over the temperature range of 1.8–300 K in an applied magnetic field of 0.01 T. The plot of $\chi_m T$ versus temperature for **5** is shown in Figure 10. At room

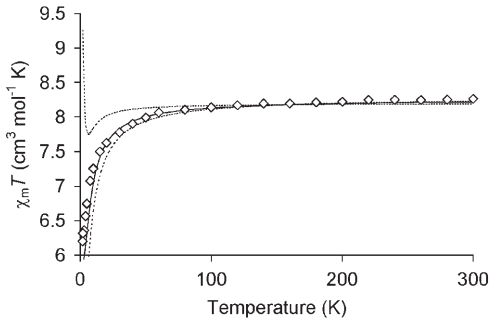

Figure 10. Plots of $\chi_m T$ versus T for **5** ($\diamond$) and the simulated fit obtained using $g_{Co\parallel}=1.98$, $g_{Co\perp}=2.21$, $g_{Gd}=1.994$, $B_{20}=-0.194$ cm^{-1} and $J_\parallel=J_\perp=-2.1$ cm^{-1}, shown as a solid line. The calculated $\chi_{\parallel m}T$ and $\chi_{\parallel m}T$ contributions obtained from the simulation are shown as dotted lines.

temperature, the experimental value of $\chi_m T$ is close to that of 8.26 $cm^3 K mol^{-1}$ predicted in the absence of significant coupling. This value decreases at low temperatures and reaches a value of 6.20 $cm^3 K mol^{-1}$ at 1.8 K, which suggests weak antiferromagnetic coupling between the $S=1/2$ and $S=7/2$ centres that results in an $S=3$ ground state, which should have a $\chi_m T$ value of 6.0 $cm^3 K mol^{-1}$.

These data can be modelled by using the isotropic spin Hamiltonian given in Equation (10), where S_{Gd} and S_{Co} are the spin operators associated with Gd^{III} and Co^{II}, and J is the magnetic exchange constant. The simplified Hamiltonian results in an expression that can be used to fit the temperature dependence of $\chi_m T$ by using the coupling constant J, as shown in Equation (11), where N represents Avogadro's number, β the Bohr Magneton, and k Boltzmann's constant. A J value of -2.1 cm^{-1} was determined from this analysis, and the modelled fit is provided in the Supporting Information. This J value corresponds to an separation of the $S=3$ ground state and the $S=4$ state of 8.4 cm^{-1}.

$$\hat{H}_{ex} = -J\hat{S}_{Gd}\cdot\hat{S}_{Co} \tag{10}$$

$$\chi_m T = \frac{4N\beta^2 g^2}{k}\left[\frac{15+7\,e^{-4J/kT}}{9+7\,e^{-4J/kT}}\right] \tag{11}$$

$$\begin{aligned}\hat{H}_{ex} = {} & g_{Gd}\beta[B_z\hat{S}_{zGd} + (1/2)(B_+\hat{S}_{-Gd} + B_-\hat{S}_{+Gd})] \\ & +\beta[g_{\parallel Co}B_z\hat{S}_{zCo} + (1/2)g_{\perp Co}(B_+\hat{S}_{-Co} + B_-\hat{S}_{+Co})] \\ & +B_{20}(\hat{S}^2_{zGd}-21/4)]-J_\parallel\hat{S}_{zGd} \\ & \cdot\hat{S}_{zCo}-(1/2)J_\perp[\hat{S}_{+Gd}\cdot\hat{S}_{-Co} + \hat{S}_{-Gd}\cdot\hat{S}_{+Co}]\end{aligned} \tag{12}$$

A more complete anisotropic Hamiltonian which accounts for the anisotropy at the Co and Gd centres is given in Equation (12), where the field in the z direction is represented by B_z, and the + and − subscripts represent raising and lowering operators, respectively ($B_\pm = B_x \pm iB_y$). The magnetic susceptibility modelled with this Hamiltonian is drawn as a solid line in Figure 10. The assumption that both $J_\parallel$ and $J_\perp$ are equal to -2.1 cm^{-1} provides a good fit; however, although the fit is strongly influenced by $J_\parallel$, small changes in $J_\perp$ do not result in large changes in the predicted temperature dependence of $\chi_m T$. The $g_{\parallel Co}$, $g_{\perp Co}$, g_{Gd} and B_{20} values used were those obtained from the analysis of the EPR spectra of complexes **3** and **4**, though the fit is also not particularly sensitive to small changes in B_{20}. The calculated $\chi_{\parallel m}T$ and $\chi_{\perp m}T$ contributions obtained from the simulation are shown as dotted lines. This analysis predicts that the lower energy $S=3$ state and higher energy $S=4$ state predicted from the isotropic model are both split by zero-field splitting, into ±3, ±2, ±1, 0 and ±4, ±3, ±2, ±1, 0 substates. The zero-field splitting of the $S=4$ state is approximately $(3/4)B_{20}$, and that of the $S=3$ state is about $(5/4)B_{20}$, in accordance with theoretically predicted values.[35] These energy levels and their field dependences are included in the Supporting Information.

The antiferromagnetic nature of the exchange coupling between Co and Gd is opposite to that most typically observed,[10,11] and provides support for the suggestion that the exchange mechanism involves direct overlap of the magnetic orbitals which contain the unpaired electrons associated with the Co^{II} and Gd^{III} centres, primarily due the extensive delocalisation of the magnetic orbitals associated with Co^{II} over the phosphorus donor. The magnitude of J found here

is comparable to values determined for other d–f heterobimetallics,[10] which demonstrates that through-space exchange coupling between transition metal and lanthanides mediated by this tripodal ligand is equally as effective as the superexchange mechanism which commonly operates in d–f complexes in which bridging donor atoms are shared by the transition metal and lanthanide. This result suggests that paramagnetic tripodal complexes of the transition metals or lanthanides with analogous supporting ligands should be effective as magnetic building blocks.

Conclusion

Even though calculations suggest that the Gd^{III} complex $[Gd\{P(CH_2NC_6H_4\text{-}2\text{-}CO_2Me)_3\}]$ has negligible spin density on the phosphorus atom, with the appropriate choice of transition metal complex it proved possible to observe magnetic exchange coupling in the heterobimetallic complex $[(TPP)Co\{P(CH_2NC_6H_4\text{-}2\text{-}CO_2Me\}_3Gd]$. This coupling is mediated by delocalisation of the spin density of the cobalt centre onto the phosphine donor, which allows direct overlap of the magnetic orbital associated with Co^{II} with the f electrons on the Gd^{III} centre. Contrary to what is typically observed in d–f complexes, where ligand superexchange pathways usually operate, this through-space interaction results in antiferromagnetic coupling. The magnitude of this exchange coupling is equal to those of other d–f complexes, which bodes well for potential use of the mononuclear lanthanide complexes of this ligand as building blocks for larger polymetallic complexes in which through-space interactions yield magnetically ordered systems or single-molecule magnet behaviour.

Experimental Section

General procedures: Unless otherwise stated, all experiments were performed under an inert atmosphere of nitrogen using either Schlenk techniques or an MBraun glove box. Dry oxygen-free solvents were used throughout. Anhydrous pentane and toluene were purchased from Aldrich, sparged with nitrogen and passed through activated alumina under a positive pressure of nitrogen gas; toluene and hexanes were further deoxygenated on Ridox catalyst columns.[36] Deuterated benzene was dried by heating at reflux over potassium in a sealed vessel under partial pressure, then trap-to-trap distilled and freeze–pump–thaw degassed three times. ^1H, $^{13}C\{^1H\}$ and $^{31}P\{^1H\}$ NMR spectra were recorded on a Bruker AMX (300 MHz) or Bruker AMX (500 MHz) spectrometer. ^1H NMR spectra were referenced to residual protons (C_6D_5H, $\delta = 7.15$) with respect to tetramethylsilane at $\delta = 0.0$. $^{13}C\{^1H\}$ spectra were referenced to solvent resonances (C_6D_6, $\delta = 128.0$). $^{31}P\{^1H\}$ NMR spectra referenced to external 85% H_3PO_4 at $\delta = 0.0$. EPR spectra of all solid samples were collected on an X-band Bruker ESR 300E spectrometer. The program Simpip[37] was used to model the Co^{II} spectra of complex **4**. The program Spin[38] was used to simulate the Gd^{3+} spectrum of **3** using only the B_{20} crystal field parameter, and the program Sim[39] was used to generate spectra with the B_{20}, B_{40} B_{43}, B_{60}, B_{63} and B_{66} crystal-field parameters. Unless otherwise noted, magnetizations were measured at 100 G with a Quantum Design Evercool MPMS-XL system. Corrections for the diamagnetic contributions of compounds were made by using Pascal's constants. Samples were run in a PVC holder specially designed to have a constant cross-sectional area. Elemental analyses were performed by the Centre for Catalysis and Materials Research (CCMR) at the University of Windsor. The compounds tris(hydroxymethyl)phosphine, methyl anthranilate, [5,10,15,20-tetrakis(4-methoxyphenyl)-21*H*,23*H*-porphine]cobalt(II) and anhydrous yttrium trichloride were purchased from Aldrich. Anhydrous $GdCl_3$ was purchased from Strem. All the reagents were used without further purification. The compounds $Y[N(SiMe_3)_2]_3$ and $Gd[N(SiMe_3)_2]_3$ were synthesised by literature methods.[40]

Synthesis of $P(CH_2NHC_6H_4\text{-}2\text{-}CO_2Me)_3$ (1): A mixture of $P(CH_2OH)_3$ (5 g, 0.040 mol), methyl anthranilate (30.45 g, 0.20 mol) and toluene (70 mL) were mixed in a 250-mL three-neck flask equipped with Dean–Stark trap and a condenser. The solution was heated to reflux for 1 h and the water produced was removed azeotropically. After cooling to room temperature the solvent was evaporated to dryness under vacuum, and the creamy white residue was rinsed with diethyl ether 2–3 times to remove excess methyl anthranilate. The product was then collected by filtration and dried under vacuum. Yield: 20 g, 95%. X-ray quality crystals were obtained by slow evaporation of a solution in benzene and hexamethyldisiloxane. ^1H NMR (C_6D_6, 300 MHz, 298 K): $\delta = 3.36$ (d, $^2J_{P,H} = 5.1$ Hz, 6H, PCH_2), 3.46 (s, 9H, CH_3), 6.49 (dd, 3H, ArH), 6.71(d, 3H, ArH), 7.15 (ddd, 3H, ArH), 7.96 (dd, 3H, ArH), 8.29 ppm (br, 3H, NH); $^{13}C\{^1H\}$ NMR (C_6D_6, 75.5 MHz, 298 K): $\delta = 38.1$ (d, $J_{P,C} = 15.4$ Hz, PCH_2), 51.1 (s, CH_3), 110.9, 112.1, 115.3, 131.9 and 134.8 (s, Ar-C), 151.6 (d, $J = 2.7$ Hz *ipso*-C), 169.1 ppm (s, CO_2); $^{31}P\{^1H\}$ NMR (C_6D_6, 121.5 MHz, 298 K): $\delta = -33.6$ ppm (s); elemental analysis calcd (%) for $C_{27}H_{30}N_3O_6P$: C 61.94, H 5.78, N 8.03; found: C 61.90, H 5.68, N 8.13.

Synthesis of $[Y\{P(CH_2NC_6H_4\text{-}2\text{-}CO_2Me)_3\}]$ (2): A mixture of $P(CH_2NHC_6H_4CO_2Me)_3$ (1.00 g, 1.91 mmol) and $[Y\{N(SiMe_3)_2\}_3]$ (1.633 g, 2.86 mmol) was stirred in toluene (70 mL) for 5 h. The resultant yellow crystalline precipitate was isolated by filtration, rinsed with 50 mL pentane and dried for 4 h (77%, 1.45 g). ^1H NMR (C_6D_6, 300 MHz, 298 K): $\delta = 3.25$ (s, 9H, CH_3), 3.92 (d, $^2J_{P,H} = 7.1$ Hz, 6H, PCH_2), 6.46 (dd, $^3J_{H,H} = 8.1$, 6.6 Hz, 3H, C_6H_4 5-H), 6.78 (d, $^3J_{H,H} = 8.8$ Hz, 3H, C_6H_4 3-H), 7.27 (ddd, $^3J_{H,H} = 8.8$, 6.6 Hz, $^4J_{H,H} = 1.8$ Hz, 3H, C_6H_4 4-H), 8.1070 ppm (dd, $^3J_{H,H} = 8.1$, $^4J_{H,H} = 1.8$ Hz, 3H, C_6H_4 6-H); $^{13}C\{^1H\}$ NMR (C_6D_6, 75.5 MHz, 298 K): $\delta = 38.1$ (d, $J_{P,C} = 15.4$ Hz, PCH_2), 51.5 (s, CH_3), 172.1 (s, CO_2), 108.7, 112.1, 114.4, 132.9 and 136.6 (s, Ar-C), 153.6 ppm (*ipso*-C); $^{31}P\{^1H\}$ NMR (C_6D_6, 121.5 MHz, 298 K): $\delta = -57.0$ ppm (d, $J_{P,Y} = 15.1$ Hz); elemental analysis calcd (%) for $C_{27}H_{27}N_3O_6PY$: C 53.21, H 4.47, N 6.90; found: C 53.10, H 4.45, N 6.96.

Synthesis of $[Gd\{P(CH_2NC_6H_4\text{-}2\text{-}CO_2Me)_3\}]$ (3): A mixture of $P(CH_2NHC_6H_4CO_2Me)_3$ (500 mg, 0.938 mmol) and $[Gd\{N(SiMe_3)_2\}_3]$ (600 mg, 0.938 mmol) was stirred in toluene (20 mL) for 30 min. The solution was filtered and remaining yellow crystalline solid was rinsed with pentane (50 mL) and dried for 4 h (67%, 425 mg). Elemental analysis calcd (%) for $C_{27}H_{27}N_3O_6PGd$: C 47.04, H 3.95, N 6.09; found: C 47.28, H 4.02, N 6.24.

Synthesis of $[(TPP)Co\{P(CH_2NC_6H_4\text{-}2\text{-}CO_2Me)_3\}Y]$ (4): A mixture of $[Y\{P(CH_2NC_6H_4\text{-}2\text{-}CO_2Me)_3\}]$ (450 mg, 0.738 mmol) and [5,10,15,20-tetrakis(4-methoxyphenyl)porphinato]cobalt(II) (584.67 mg, 0.737 mmol) was stirred in toluene (25 mL) for 30 min. The solution was filtered and the resultant reddish-purple crystalline solid was washed with pentane (50 mL) and dried for 4 h (65.2%, 675 mg). X-ray quality crystals were obtained by performing the reaction without stirring, and the structure contained 2 equivalents of co-crystallised toluene. The complex is sparingly soluble in toluene and benzene. ^1H NMR (C_6D_6, 300 MHz, 298 K): $\delta = 3.2$ (br, 9H, CO_2CH_3), 4.4 (br, 18H total, OCH_3 and PCH_2), 5.8 (br, 3H, C_6H_4), 6.9 (br, 3H, C_6H_4), 7.3 (br, 3H, C_6H_4), 8.2 (br, 3H, C_6H_4), 8.8 (br, 8H, TPP *m*-*H*), 11.5 (vbr, 8H, TPP *o*-*H*), 15.1 ppm (v br, 8H, pyrrole H); elemental analysis calcd (%) for $C_{75}H_{63}N_7O_{10}PYCo$: C 64.29, H 4.53, N 7.00; found: C 64.23, H 4.82, N 6.81.

Synthesis of $[(TPP)Co\{P(CH_2NC_6H_4\text{-}2\text{-}CO_2Me)_3\}Gd]$ (5): A mixture of $[Gd\{P(CH_2NC_6H_4\text{-}2\text{-}CO_2Me)_3\}]$ (500 mg, 0.737 mmol) and [5,10,15,20-tetrakis(4-methoxyphenyl)porphinato]cobalt(II), $[Co^{II}(TPP)]$ (584 mg, 0.737 mmol) was stirred in toluene (25 mL) for 30 min. The solution was filtered and the resultant reddish purple crystalline solid was washed with pentane (50 mL) and dried for 3–4 h (47.5%, 515 mg); elemental analysis

Table 1. X-ray crystallographic data for **1**–**5**.

	1	**2**	**3**	**4**	**5**
empirical formula	$C_{30}H_{33}N_3O_6P$	$C_{27}H_{27}N_3O_6PY$	$C_{27}H_{27}N_3O_6PGd$	$C_{89}H_{79}N_7O_{10}PCoGd$	$C_{89}H_{79}N_7O_{10}PCoY$
formula weight	562.56	609.40	708.7	1653.74	1585.46
crystal system	triclinic	trigonal	trigonal	triclinic	triclinic
a [Å]	10.8108(17)	14.6660(3)	14.6765(11)	14.442(2)	14.4404(19)
b [Å]	11.3382(18)	14.6660(3)	14.6660(11)	15.495(2)	15.509(2)
c [Å]	12.513(2)	20.9460(9)	21.2161(3)	18.737(3)	18.736(2)
α [°]	104.725(2)	90	90	90.648(2)	90.2840(10)
β [°]	104.725(2)	90	90	112.571(2)	112.6130(10)
γ [°]	90.718(2)	120	120	89.894(2)	90.1050(10)
V [Å^3]	1429.3(4)	3905.06(20)	3957.7(7)	3871.5(10)	3873.5(10)
space group	$P\bar{1}$	$R3c$	R3c	$P\bar{1}$	$P\bar{1}$
Z	2	6	6	2	2
ρ_{calcd} [g cm^{-1}]	1.31	1.56	1.70	1.36	1.42
$\mu(Mo_{K\alpha})$ [mm^{-1}]	0.144	2.349	2.684	1.150	1.046
T [K]	173	173	173	173	173
$2\theta_{max}$ [°]	50.0	50.0	50.0	55.0	52.5
min./max. transmission	0.9473/0.9420	0.791/0.584	not fully solved[a]	0.708/0.811	0.818/0.977
total reflns	16454	13993	13580	43148	44292
unique reflns (residue)	6348 (R_{int} = 0.0439)	1530 (R_{int} = 0.0867)	1999 (R_{int} = 0.0821)	17077 (R_{int} = 0.0323)	7230 (R_{int} = 0.0258)
parameters	356	39	not fully solved[a]	991	991
$R1$; $wR2$ (all data)	0.0624; 0.1800	0.1372; 0.4167[a]	not fully solved[a]	0.0397; 0.1115	0.0391; 0.1041

[a] Twinning complicated solutions of structures for **2** and **3**.

calcd (%) for $C_{75}H_{63}N_7O_{10}PGdCo$: C 61.30, H 4.32, N 6.67; found: C 61.47, H 4.12, N 6.54.

X-ray crystallography: Each crystal was covered with Paratone, mounted on a glass fibre and rapidly placed into the cold N_2 stream of the Kryo-Flex low-temperature device. The data were collected using SMART[41] software on a Bruker APEX CCD diffractometer with graphite-monochromated $Mo_{K\alpha}$ radiation (λ = 0.71073 Å). Details of crystal data, data collection and structure refinement are listed in Table 1. Data reduction was performed using SAINT[42] software, and the data were corrected for absorption using SADABS.[43] The structures were solved by direct methods using SIR97[44] and refined by full-matrix least-squares on F^2 using SHELXL-97[45] and the WinGX[46] software package, and the thermal ellipsoid plots were produced using ORTEP32.[47] In general, thermal parameters for non-hydrogen atoms were treated anisotropically, and all hydrogen atoms were placed in idealised locations. The co-crystallised benzene solvent in **1** was modelled as an idealised hexagon, with equal isotropic thermal parameters on the six carbon atoms, and the hydrogen atoms associated with this disordered moiety were omitted. The hydrogen atoms associated with the three amino groups that were involved in hydrogen bonding in **1** were located in an electron-density difference map and their positions and isotropic thermal parameters were refined. Multiple data sets were acquired for complexes **2** and **3**, but all suffered from twinning. All atoms in the solution for **2** were treated isotropically and the arene ring was modelled as a perfect hexagon with each carbon bearing identical thermal parameters. Only the P and Gd centres were readily located in the attempted solution of the structure of **3**.

CCDC-638601 (**1**), CCDC-638602 (**2**), CCDC-638603 (**4**) and CCDC-638604 (**5**) contain the supplementary crystallographic data for this paper. These data can be obtained free of charge from The Cambridge Crystallographic Data Centre via www.ccdc.cam.ac.uk/data_request/cif.

Calculations: Ab initio DFT calculations were performed by using the hybrid-functional B3LYP or UB3LYP[48] method with the Gaussian 03 package.[49] The basis functions used were the DGDZVP set for complex **2**, and CEP-31G for complex **3**. Both were optimised with C_3 symmetry. For the model complex of **4** the CEP-121G* basis set was used on all atoms except for Y and Co, for which the CEP-121G basis set was used. All these basis sets are provided in the Gaussian 03 program suite.

Acknowledgements

Acknowledgement is made to the National Sciences and Engineering Research Council (NSERC) of Canada and the Ontario Research and Development Challenge Fund (ORDCF) for their financial support.

[1] a) K. Itoh, M. Kinoshita, *Molecular Magnetism: New Magnetic Materials*, Taylor & Francis, London, **2002**; b) O. Kahn, *Molecular Magnetism*, VCH, Weinheim, **1993**; c) R. Jain, K. Kabir, J. B. Gilroy, K. A. R. Mitchell, K.-C. Wong, R. G. Hicks, *Nature* **2007**, *445*, 291–294.

[2] J. S. Miller, *Dalton Trans.* **2006**, 2742–2749.

[3] J. S. Miller, A. J. Epstein, *Angew. Chem.* **1994**, *106*, 399–432; *Angew. Chem. Int. Ed. Engl.* **1994**, *33*, 385–415.

[4] J. Mrozinski, *Coord. Chem. Rev.* **2005**, *249*, 2534–2548.

[5] L. M. C. Beltran, J. R. Long, *Acc. Chem. Res.* **2005**, *38*, 325–334.

[6] a) D. Li, S. Parkin, G. Wang, G. T. Yee, R. Clerac, W. Wernsdorfer, S. M. Holmes, *J. Am. Chem. Soc.* **2006**, *128*, 4214–4215; b) C. P. Berlinguette, D. Vaughn, C. Canada-Vilalta, J. R. Galan-Mascaros, K. R. Dunbar, *Angew. Chem.* **2003**, *115*, 1561–1564; *Angew. Chem. Int. Ed.* **2003**, *42*, 1523–1526.

[7] a) O. Kahn, *NATO Adv. Study Inst. Ser. Ser. C* **1997**, *499*, 287–302; b) L. M. Toma, L. D. Toma, F. S. Delgado, C. Ruiz-Perez, J. Sletten, J. Cano, J. M. Clemente-Juan, F. Lloret, M. Julve, *Coord. Chem. Rev.* **2006**, *250*, 2176–2193; c) T. E. Vos, J. S. Miller, *Angew. Chem.* **2005**, *117*, 2468–2471; *Angew. Chem. Int. Ed.* **2005**, *44*, 2416–2419; d) S. Tanase, J. Reedijk, *Coord. Chem. Rev.* **2006**, *250*, 2501–2510; e) B. D. Koivisto, R. G. Hicks, *Coord. Chem. Rev.* **2005**, *249*, 2612–2630; f) H. Miyasaka, R. Clerac, *Bull. Chem. Soc. Jpn.* **2005**, *78*, 1725–1748; g) M. Pilkington, S. Decurtins, *Persp. Supramol. Chem.* **2003**, *7*, 275–323.

[8] a) J. A. Hatnean, R. Raturi, J. Lefebvre, D. B. Leznoff, G. Lawes, S. A. Johnson, *J. Am. Chem. Soc.* **2006**, *128*, 14992–14999; b) A. L. Keen, M. Doster, H. Han, S. A. Johnson, *Chem. Commun.* **2006**, 1221–1223; c) H. Han, S. A. Johnson, *Organometallics* **2006**, *25*, 5594–5602.

[9] H. Han, M. Elsmaili, S. A. Johnson, *Inorg. Chem.* **2006**, *45*, 7435–7445.

[10] a) M. Sakamoto, K. Manseki, H. Okawa, *Coord. Chem. Rev.* **2001**, *219–221*, 379–414; b) C. Benelli, D. Gatteschi, *Chem. Rev.* **2002**, *102*, 2369–2387.
[11] a) A. Bencini, C. Benelli, A. Caneschi, R. L. Carlin, A. Dei, D. Gatteschi, *J. Am. Chem. Soc.* **1985**, *107*, 8128–8136; b) C. Benelli, A. Caneschi, D. Gatteschi, O. Guillou, L. Pardi, *Inorg. Chem.* **1990**, *29*, 1750–1755; c) M. Sasaki, K. Manseki, H. Horiuchi, M. Kumagai, M. Sakamoto, H. Sakiyama, Y. Nishida, M. Sakai, Y. Sadaoka, M. Ohba, H. Okawa, *J. Chem. Soc. Dalton Trans.* **2000**, 259–263; d) J.-P. Costes, F. Dahan, B. Donnadieu, J. Garcia-Tojal, J.-P. Laurent, *Eur. J. Inorg. Chem.* **2001**, 363–365; e) N. Matsumoto, M. Sakamoto, H. Tamaki, H. Okawa, S. Kida, *Chem. Lett.* **1990**, 853–854; f) M. Andruh, I. Ramade, E. Codjovi, O. Guillou, O. Kahn, J. C. Trombe, *J. Am. Chem. Soc.* **1993**, *115*, 1822–1829; g) A. J. Blake, R. O. Gould, C. M. Grant, P. E. Y. Milne, S. Parsons, R. E. P. Winpenny, *J. Chem. Soc. Dalton Trans.* **1997**, 485–495; h) J.-P. Costes, M. Auchel, F. Dahan, V. Peyrou, S. Shova, W. Wernsdorfer, *Inorg. Chem.* **2006**, *45*, 1924–1934; i) J.-P. Costes, F. Dahan, A. Dupuis, J.-P. Laurent, *Inorg. Chem.* **1996**, *35*, 2400–2402; j) C. Benelli, A. J. Blake, P. E. Y. Milne, J. M. Rawson, R. E. P. Winpenny, *Chem. Eur. J.* **1996**, *1*, 614–618; k) X.-M. Chen, Y.-L. Wu, Y.-X. Tong, X.-Y. Huang, *J. Chem. Soc. Dalton Trans.* **1996**, 2443–2448; l) J. F. Petit, J. C. Trombe, A. Gleizes, J. Galy, *C. R. Acad. Sci. Ser. II* **1987**, *304*, 1117–1120; m) R. Kempe, H. Noss, T. Irrgang, *J. Organomet. Chem.* **2002**, *647*, 12–20; n) R. Koner, H.-H. Lin, H.-H. Wei, S. Mohanta, *Inorg. Chem.* **2005**, *44*, 3524–3536; o) J.-P. Sutter, M. L. Kahn, *Magnetism: Molecules to Materials V*, Wiley-VCH, Weinheim, **2005**, pp. 161–187.
[12] C. M. Zaleski, E. C. Depperman, J. W. Kampf, M. L. Kirk, V. L. Pecoraro, *Angew. Chem.* **2004**, *116*, 4002–4004; *Angew. Chem. Int. Ed.* **2004**, *43*, 3912–3914.
[13] F. Pointillart, K. Bernot, R. Sessoli, D. Gatteschi, *Chem. Eur. J.* **2007**, *13*, 1602–1609.
[14] V. S. Mironov, Y. G. Galyametdinov, A. Ceulemans, C. Gorller-Walrand, K. Binnemans, *J. Chem. Phys.* **2002**, *116*, 4673–4685.
[15] a) A. Mishra, W. Wernsdorfer, S. Parsons, G. Christou, E. K. Brechin, *Chem. Commun.* **2005**, 2086–2088; b) A. Mishra, W. Wernsdorfer, K. A. Abboud, G. Christou, *J. Am. Chem. Soc.* **2004**, *126*, 15648–15649; c) S. Osa, T. Kido, N. Matsumoto, N. Re, A. Pochaba, J. Mrozinski, *J. Am. Chem. Soc.* **2004**, *126*, 420–421; d) M. Ferbinteanu, T. Kajiwara, K.-Y. Choi, H. Nojiri, A. Nakamoto, N. Kojima, F. Cimpoesu, Y. Fujimura, S. Takaishi, M. Yamashita, *J. Am. Chem. Soc.* **2006**, *128*, 9008–9009; e) J. Tang, I. Hewitt, N. T. Madhu, G. Chastanet, W. Wernsdorfer, C. E. Anson, C. Benelli, R. Sessoli, A. K. Powell, *Angew. Chem.* **2006**, *118*, 1761–1765; *Angew. Chem. Int. Ed.* **2006**, *45*, 1729–1733; f) G. Christou, D. Gatteschi, D. N. Hendrickson, R. Sessoli, *MRS Bull.* **2000**, *25*, 66–71; g) J.-P. Costes, F. Dahan, W. Wernsdorfer, *Inorg. Chem.* **2006**, *45*, 5–7.
[16] A. W. Frank, G. L. Drake, Jr., *J. Org. Chem.* **1972**, *37*, 2752–2755.
[17] K. W. Feindel, R. E. Wasylishen, *Can. J. Chem.* **2004**, *82*, 27–44.
[18] M. D. Fryzuk, T. S. Haddad, D. J. Berg, *Coord. Chem. Rev.* **1990**, *99*, 137–212.
[19] a) S. O. Grim, S. A. Sangokoya, *J. Chem. Soc. Chem. Commun.* **1984**, 1599–1600; b) A. A. Pinkerton, W. L. Earl, *J. Chem. Soc. Dalton Trans.* **1979**, 1347–1349.
[20] R. Stowasser, R. Hoffmann, *J. Am. Chem. Soc.* **1999**, *121*, 3414–3420.
[21] C. A. Hutchison, Jr., B. R. Judd, D. F. D. Pope, *Proc. Phys. Soc. B* **1957**, *70*, 514–520.
[22] N. Ishikawa, N. Tanaka, Y. Kaizu, *Inorg. Chim. Acta* **2004**, *357*, 2181–2184.
[23] N. Ishikawa, M. Sugita, W. Wernsdorfer, *Angew. Chem.* **2005**, *117*, 2991–2995; *Angew. Chem. Int. Ed.* **2005**, *44*, 2931–2935.
[24] N. Ishikawa, M. Sugita, W. Wernsdorfer, *J. Am. Chem. Soc.* **2005**, *127*, 3650–3651.
[25] a) B. B. Wayland, M. E. Abd-Elmageed, *J. Am. Chem. Soc.* **1974**, *96*, 4809–4814; b) B. B. Wayland, J. V. Minkiewixz, M. E. Abd-Elmageed, *J. Am. Chem. Soc.* **1974**, *96*, 2795–2801; c) B. De Castro, M. Rangel, J. B. Raynor, *J. Chem. Soc. Dalton Trans.* **1990**, 3311–3318.
[26] M. D. Fryzuk, D. B. Leznoff, R. C. Thompson, S. J. Rettig, *J. Am. Chem. Soc.* **1998**, *120*, 10126–10135.
[27] D. C. Bradley, M. B. Hursthouse, R. J. Smallwood, A. J. Welch, *J. Chem. Soc. Chem. Commun.* **1972**, 872.
[28] R. D. Shannon, *Acta. Crystallogr. Sect. A* **1976**, *32*, 751–767.
[29] P. B. Hitchcock, M. F. Lappert, I. A. MacKinnon, *J. Chem. Soc. Chem. Commun.* **1988**, 1557–1558.
[30] P. W. Roesky, M. T. Gamer, N. Marinos, *Chem. Eur. J.* **2004**, *10*, 3537–3542.
[31] B. R. McGarvey, *Can. J. Chem.* **1975**, *53*, 2498–2511.
[32] W. C. Lin, *Inorg. Chem.* **1976**, *15*, 1114–1118.
[33] B. B. Wayland, A. E. Sherry, A. G. Bunn, *J. Am. Chem. Soc.* **1993**, *115*, 7675–7684.
[34] B. R. McGarvey, *J. Phys. Chem.* **1967**, *71*, 51–66.
[35] J. Owen, *J. Appl. Phys.* **1961**, *32*, S213–217.
[36] A. B. Pangborn, M. A. Giardello, R. H. Grubbs, R. K. Rosen, F. J. Timmers, *Organometallics* **1996**, *15*, 1518–1520.
[37] Simpip, An EPR simulation program, M. Nilges, Illinois EPR Research Centre.
[38] Spin, EPR simulation program, A. Ozarowski, National High Magnetic Field Laboratory, Florida.
[39] Sim, version 2004-5, An EPR Simulation Program, H. Weihe, Department of Chemistry, University of Copehagen.
[40] a) D. C. Bradley, J. S. Ghotra, F. A. Hart, *J. Chem. Soc. Chem. Commun.* **1972**, 349–350; b) D. C. Bradley, J. S. Ghotra, F. A. Hart, *J. Chem. Soc. Dalton Trans.* **1973**, 1021–1023.
[41] SMART, Molecular analysis research tool, Bruker AXS Inc., Madison, WI, **2001**.
[42] SAINTPlus, Data reduction and correction program′; Bruker AXS Inc.: Madison, WI, **2001**.
[43] SADABS, An empirical absorption correction program, Bruker AXS Inc., Madison, WI, **2001**.
[44] A. Altomare, M. C. Burla, M. Camalli, G. L. Cascarano, C. Giacovazzo, A. Guagliardi, A. G. G. Moliterni, G. Polidori, R. Spagna, *J. Appl. Crystallogr.* **1999**, *32*, 115–119.
[45] Sheldrick, G. M. SHELXL-97, Universitat Gottingen: Gottingen, **1997**.
[46] L. J. Farrugia, *J. Appl. Crystallogr.* **1999**, *32*, 837–838.
[47] L. J. Farrugia, *J. Appl. Crystallogr.* **1997**, *30*, 565.
[48] A. D. Becke, *J. Chem. Phys.* **1993**, *98*, 5648–5652.
[49] Gaussian 03, Revision C.01, M. J. Frisch, G. W. Trucks, H. B. Schlegel, G. E. Scuseria, M. A. Robb, J. R. Cheeseman, J. A. Montgomery, Jr., T. Vreven, K. N. Kudin, J. C. Burant, J. M. Millam, S. S. Iyengar, J. Tomasi, V. Barone, B. Mennucci, M. Cossi, G. Scalmani, N. Rega, G. A. Petersson, H. Nakatsuji, M. Hada, M. Ehara, K. Toyota, R. Fukuda, J. Hasegawa, M. Ishida, T. Nakajima, Y. Honda, O. Kitao, H. Nakai, M. Klene, X. Li, J. E. Knox, H. P. Hratchian, J. B. Cross, V. Bakken, C. Adamo, J. Jaramillo, R. Gomperts, R. E. Stratmann, O. Yazyev, A. J. Austin, R. Cammi, C. Pomelli, J. W. Ochterski, P. Y. Ayala, K. Morokuma, G. A. Voth, P. Salvador, J. J. Dannenberg, V. G. Zakrzewski, S. Dapprich, A. D. Daniels, M. C. Strain, O. Farkas, D. K. Malick, A. D. Rabuck, K. Raghavachari, J. B. Foresman, J. V. Ortiz, Q. Cui, A. G. Baboul, S. Clifford, J. Cioslowski, B. B. Stefanov, G. Liu, A. Liashenko, P. Piskorz, I. Komaromi, R. L. Martin, D. J. Fox, T. Keith, M. A. Al-Laham, C. Y. Peng, A. Nanayakkara, M. Challacombe, P. M. W. Gill, B. Johnson, W. Chen, M. W. Wong, C. Gonzalez, J. A. Pople, Gaussian, Inc., Wallingford CT, **2004**..

Received: March 2, 2007
Revised: October 3, 2007
Published online: November 14, 2007

